

Article

Performance of Burn-Severity Metrics and Classification in Oak Woodlands and Grasslands

Michael C. Stambaugh ^{1,*}, Lyndia D. Hammer ² and Ralph Godfrey ³

¹ Department of Forestry, 203 ABNR Building, University of Missouri-Columbia, Columbia, MO 65211, USA

² Lomakatsi Restoration Project, PO Box 3084, Ashland, OR 97520, USA;
E-Mail: lyndiahammer@gmail.com

³ Wichita Mountains Wildlife Refuge, U.S. Fish and Wildlife Service, 32 Refuge Headquarters, Indianola, OK 73552, USA; E-Mail: rgodfrey@fws.gov

* Author to whom correspondence should be addressed; E-Mail: stambaughm@missouri.edu;
Tel.: +1-573-882-8841; Fax: +1-573-882-1977.

Academic Editors: Ioannis Gitas, Josef Kellndorfer and Prasad S. Thenkabail

Received: 1 April 2015 / Accepted: 12 August 2015 / Published: 17 August 2015

Abstract: Burn severity metrics and classification have yet to be tested for many eastern U.S. deciduous vegetation types, but, if suitable, would be valuable for documenting and monitoring landscape-scale restoration projects that employ prescribed fire treatments. Here we present a performance analysis of the Composite Burn Index (CBI) and its relationship to spectral data (differenced Normalized Burn Ratio (dNBR) and its relative form (RdNBR)) across an oak woodland - grassland landscape in southwestern Oklahoma, USA. Correlation and regression analyses were used to compare CBI strata, assess models describing burn severity, and determine thresholds for burn severity classes. Confusion matrices were used to assess burn severity classification accuracy. Our findings suggest that dNBR and RdNBR, thresholded using total CBI, can produce an accurate burn severity map in oak woodlands, particularly from an initial assessment period. Lower accuracies occurred for burn severity classifications of grasslands and raises questions related to definitions and detection of burn severity for grasslands, particularly in transition to more densely treed structures such as savannas and woodlands.

Keywords: CBI; drought; fire history; Landsat; dNBR; RdNBR; remote sensing

1. Introduction

Despite burn severity metrics and classification through remote sensing being used throughout the world [1–4], they have yet to be described for many eastern U.S. vegetation types, such as deciduous forests. The ability to describe, quantify, and remotely sense burn severity in this region would be particularly useful for documentation, monitoring, and prioritization of landscape-scale restoration projects that include prescribed burning [5]. In the last decade, research on fire regime characteristics and post-fire effects has included increased emphasis on understanding the importance of the full range of burn severities in forest ecosystems [6–8]. The role of mixed- to high-severity fire has been of particular interest, both in wildfire and prescribed fire contexts [9–11].

Burn severity describes fire effects on above-ground vegetation and soil organic matter [12,13]. From field measures to remote sensing and modeling, assessing burn severity presents diverse challenges [14]. Within remote sensing, various data (e.g., optical, RADAR, LiDAR) and approaches for assessing burned areas exist [15–17]. Burn severity assessments have attempted to develop predictive models relating multispectral satellite data to field measured burn severity measures [18], compare conceptual historical fire regimes to current fire regimes [19], evaluate effectiveness of fuel treatments [20,21], and monitor trends over time [22,23]. In relation to forest ecology and management, burn severity data can be used to measure severity by vegetation type(s), project forest successional trajectories, and contribute to modeling second-order fire effects [24,25].

FIREMON Landscape Assessment [26] is a standardized burn severity monitoring approach that allows measuring and mapping burn severity from a combination of remotely sensed vegetation change and ground-based plot data, although other burn severity assessment techniques are capable of providing spatial data needed to support pre- and post-fire management decisions and monitoring [27,28]. A commonly used technique utilizes the magnitude of change in reflected electromagnetic (EM) radiation between pre-fire and post-fire landscape conditions. The spectral response curve of typical vegetation occurs from 0.4 to 2.5 μm . A relatively high green reflectance response occurs due to chlorophyll pigmentation in the visible range. A high near infrared (NIR; reflected infrared) response occurs due to healthy plant cell structure and shortwave-infrared (SWIR; partly reflected, partly emitted) has a relatively low response due to moisture absorption.

The Landsat satellite collects multispectral EM data divided into spectral bands. Landsat Band 4 measures radiance in the NIR range and Band 7 has sensitivity in the SWIR range. The band ratio between Band 4 (healthy vegetation) and Band 7 (burned area; increased cover of bare soil and ash, decreased greenness, and reduced plant moisture content) are commonly used for burn severity mapping [29]. This change metric is at the resolution of the remote sensing imagery (e.g., 30 m) and, as a result, the effects on the ground specific to trees, plants and soil are averaged to imagery resolution. In many cases, imagery resolution limits visibility of finer-scale variation of fire effects and a bridge is needed between the ground level and remotely sensed scales to help define the meaning of a range of severity scores across the landscape [29]. To this end, the Composite Burn Index (CBI) field protocol [26] was developed to enable “ground truthing” or definition of burn severity conditions at the plot level, to enable adjustment of the severity score at the resolution of imagery, and to understand the ground-level effects described by the severity classification across the landscape. CBI rates burn effects from the soil to the upper canopy layers and then averages those ratings to derive a plot-level index value (*i.e.*, CBI). Rating factors

include changes to soil color, fuels consumed, stem char, vegetation mortality and resprouting, and changes in plant community composition [26]. Rating factors were designed to describe ecological attributes of change and correlate with changes detected by multispectral satellite imagery [26]. CBI has been tested and used to validate burn severity maps in many ecosystems [13,30,31], but has not been tested specifically in open-canopy structured oak woodlands of the eastern U.S. The objectives of this research were to: (1) describe burn severity in this community type using the CBI protocol; and (2) gauge the performance of satellite imagery to map burn severity across a gradient of grasslands and oak woodlands by considering differences in land-types, CBI strata, and remotely-sensed burn severity metrics.

2. Data and Methods

2.1. Study Site

The study site was located in the Wichita Mountains Wildlife Refuge (WMWR) at the western edge of the Cross Timbers region in southwestern Oklahoma, Comanche County, USA (Figure 1). Mountain peaks are surrounded by a matrix of mixed-grass prairie with wooded lower slopes and creeks forming an intermediate zone between the relatively flat valley floor and the steep, rocky slopes. Elevations range from 411 m asl to 756 m asl. Three major land-types (grasslands, woodlands, and rock outcrops) occupy 98.5% of the refuge area.

The WMWR serves as an important ecotone for eastern and western plant and animal species. Dominant trees are post oak (*Quercus stellata*), blackjack oak (*Quercus marilandica*) and eastern redcedar (*Juniperus virginiana*), and dominant grasses include little bluestem (*Schizachyrium scoparium*), big bluestem (*Andropogon gerardii*) and hairy grama (*Bouteloua hirsuta*) [32]. Southwestern Oklahoma, encompassing the Wichita Mountains, is characterized by a continental, temperate climate with a mean annual temperature of 16.1 degrees Celsius (Period: 1895–2011; National Climatic Data Center, Division 7, SW Oklahoma) and 78 cm average annual rainfall (period: 1914–2008) [33].

Since the beginning of the 20th century, the landscape of the WMWR has been transitioning towards more forested conditions and increased eastern redcedar density primarily due to altered fire regimes [34,35]. Starting 29 January 2010, one of the most destructive ice storms of local record caused significant damage to overstory trees and, consequently, large increases in woody fuel loadings. From about July 2010, much of the southern plains had experienced severe to exceptional drought conditions (*i.e.*, Palmer Drought Severity Index (PDSI) ≤ -3.0). Beginning in May 2011, drought conditions were extreme (PDSI < -4.0) for much of southwestern Oklahoma. The Ferguson Fire of September 2011 burned a large portion of the WMWR and resulted in a wide range of fire severities. The Ferguson Fire started 1 September 2011 during exceptional drought conditions and continued until 7 September 2011, with a total of 16,150 hectares burned (Figure 1). Moisture contents of 1000-h fuels were recorded at 3% by WMWR fire staff. Though drought conditions eased during spring of 2012, southwestern Oklahoma continued to be moderately to exceptionally dry until summer 2015 [36]. Persistent drought conditions following the Ferguson Fire likely accentuated the observed fire effects.

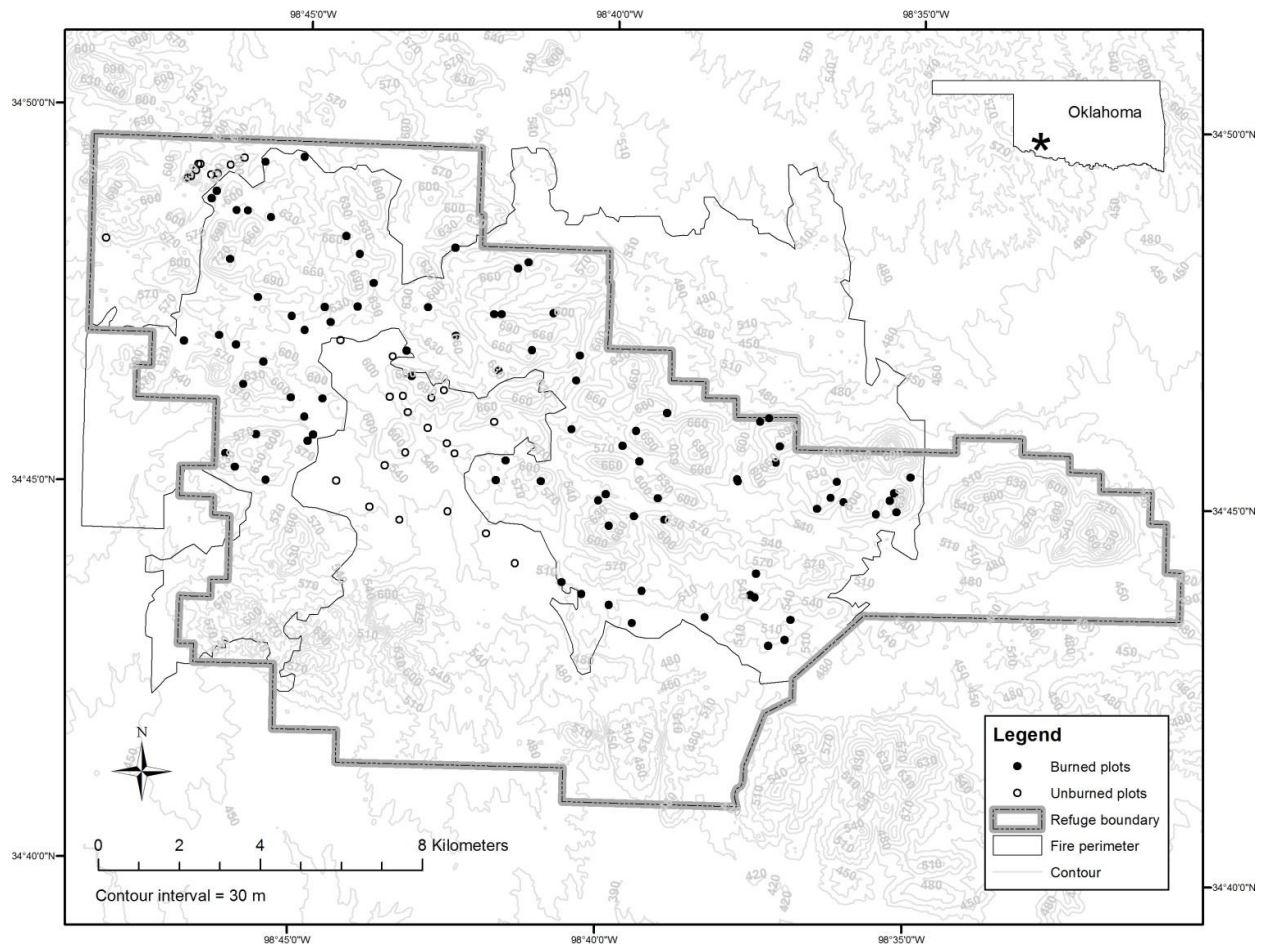


Figure 1. Topographic map of the Wichita Mountains Wildlife Refuge (WMWR) showing the perimeter of the Ferguson Fire and locations of plots used to measure post-fire vegetation and burn severity. Asterisk on inset map of Oklahoma indicates location of the study area.

2.2. Sampling Design

Prior to the Ferguson Fire, 343 vegetation plots (706 m²) were sampled across WMWR. Plot locations were randomly generated in GIS (ArcView 3.2; ESRI) and then realigned to the center of the associated 30-meter grid cell of a digital elevation model (DEM) [37]. Plot vegetation was classified into three land-types following Hoagland's [38] Oklahoma vegetation community type definitions with minor modification: (1) woodland: $\geq 25\%$ deciduous tree cover; (2) grassland: $>25\%$ combined grass and forb cover, and $<25\%$ deciduous tree cover; and (3) rocky: $>25\%$ rock cover and $<25\%$ deciduous or grassland cover.

Following the Ferguson Fire, we re-measured 120 plots (Figure 1). This resampling effort was timed with the production of the Monitoring Trends in Burn Severity (MTBS) Extended Assessment for the Ferguson Fire. The MTBS project utilizes Landsat multispectral data and the differenced Normalized Burn Ratio algorithm (dNBR, Equation (2)) to produce burn severity maps for all large fires in the US, significantly aiding the efforts of land managers and researchers in assessment of fire effects [39]. Criteria for re-measurement of vegetation plots were: (1) located within the Landsat 7 dataset (*i.e.*, not included in strips of “no data” resulting from a known Scan Line Corrector error (see Figure 2)); (2) photographed prior to the fire; (3) evenly distributed among burn severity classes (unburned, low,

moderate, and high) (Figure 2); (4) located within a relatively homogenous burn severity “patch”; (5) distributed among land-types (grassland, rocky, and woodland); and (6) readily accessible. To locate plots on the ground, we utilized GPS locations (3 m horizontal accuracy) followed by geo-rectification from four pre-fire photographs taken from plot center. Plots were stratified by severity using the classified, extended assessment (EA) (Table 1) differenced Normalized Burn Ratio (dNBR) dataset produced by the USGS Center for Earth Resources Observation and Science (EROS) for the MTBS project in July 2012. Landsat pair acquisition and processing followed MTBS EA protocols and was timed to detect maximum greenness one growing season post-fire, coincided with our season of survey, and was constrained by cloud, dust, and smoke-free atmospheric conditions [39]. We expected that utilizing the extended assessment (EA) data, as compared to the Initial Assessment (IA) data, would enable accounting for delayed mortality or survival of vegetation and better characterize the longer-term ecological response to burn severity [26]. Additionally, based on observations by WMWR biologists, the EA classified dNBR severity map more closely matched the visually detected effects on canopy trees than did the classified initial assessment severity map.

Thirty plots were resampled in each burn severity class. Focal statistics analysis (Spatial Analyst, ArcGIS 10.0) on a 3×3 neighborhood identified the range (minimum – maximum) of dNBR values and was used to select plots located in relatively homogeneous burn severity patches. Previous work by Key and Benson [26] suggested that sampling within a patch of uniform burn severity was useful for refining relationships among remotely sensed data and CBI. Due to the offset between the circular vegetation plot coverage and the center of each grid cell, bilinear interpolation was used with the Spatial Analyst Extract (ArcGIS 10.0) tool to assign dNBR and Relative differenced Normalized Burn Ratio (RdNBR) values to plots. Bilinear interpolation considered the average value of the four nearest adjacent cells, while the no interpolation option gives the value of the grid cell containing the center point. Because plots may not always be located exactly at the center point of a grid cell, point scores could differ from half or more of the plot score. Thus, the interpolation option was expected to improve the correlation between CBI and burn ratios based on a comparable study [30] that found that bilinear interpolation performed better than using the nearest neighbor average or a distance-weighted averaging method of 16 surrounding cells.

2.3. Composite Burn Index (CBI)

CBI measurements followed methods of Key and Benson [26] with scores generated for five strata: (1) substrate; (2) herbs, low shrubs and trees <1-m tall (termed “grass stratum” in remainder of document); (3) tall shrubs and trees (1 to 5 m tall; termed “shrub stratum” in remainder of document); (4) short trees; and (5) tall trees. Due to the short stature of trees in the Cross Timbers and at the WMWR, we modified tree height ranges measured in each stratum resulting in “short trees” ranging from 3 to 9 m tall, and “tall trees” being >9 m tall. Tree height was the only modification we made to the CBI protocol. Trees were scored based on the total change to foliage as green, scorched or torched, percent canopy mortality, and total char height.

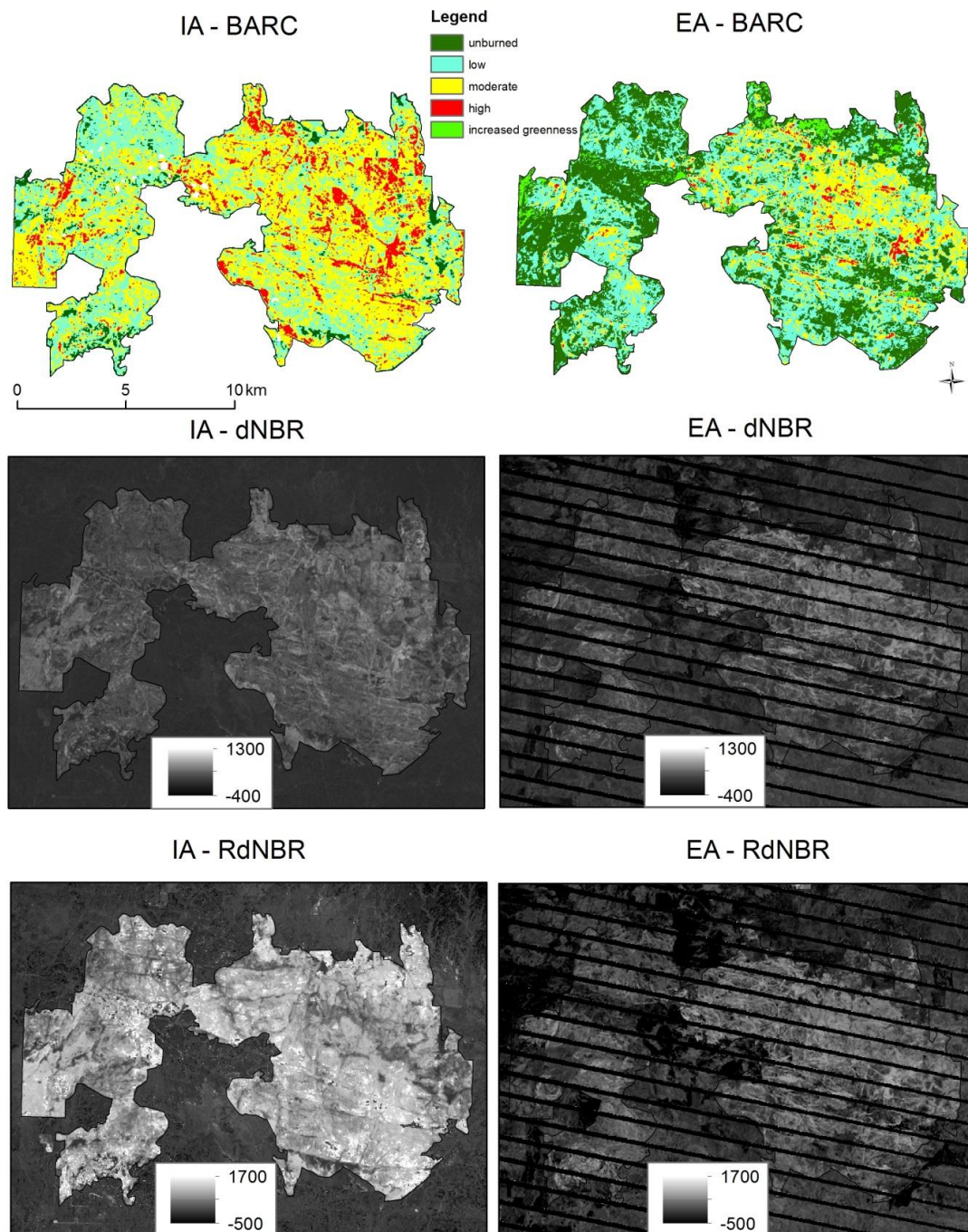


Figure 2. Maps of burn severity classification produced by the Burned Area Emergency Response (BAER) and MTBS projects for the Ferguson Fire. Thematically classified Burned Area Reflectance Classification (BARC) maps are produced for both a rapid initial assessment (IA) of burn severity within approximately one month following the fire and, for an extended assessment (EA) of burn severity, one growing season following the fire [39]. Thematically classified maps are produced using the dNBR (Equation 2) without the use of CBI plot data. See Table 1 for timing of the IA and EA. Stripes of “no data” resulting from a Landsat 7 scan line corrector (SLC) error were filled by MTBS analysts for the production of the thematically classified map, however, plot data analyzed by this study were not affected by the SLC error.

Table 1. Data collection dates and methods for vegetation plots, the composite burn index (CBI), and satellite imagery-based initial and extended assessments of fire severity.

Data	Collection Date(s)	Sampling Method
Pre-fire vegetation	3/2010 to 6/2011	15 m radius plots
Post-fire vegetation	8/2012	15 m radius plots
Composite Burn Index	8/2012	15 m radius plots
Pre-fire imagery-Initial Assessment	8/17/2011	Landsat 5 TM
Post-fire imagery-Initial Assessment	10/04/2011	Landsat 5 TM
Pre-fire imagery-Extended Assessment	5/29/2011	Landsat 5 TM
Post-fire imagery-Extended Assessment	5/23/2012	Landsat 7 ETM+

2.4. Satellite Imagery and Pre-Processing

The normalized burn ratio (NBR) was calculated as:

$$NBR = (TM4 - TM7) / (TM4 + TM7) \times 1000 \quad (1)$$

where TM4 and TM7 are the pixel surface spectral reflectance intensities of the Landsat Band 4 (0.76 to 0.90 μm , near-infrared) and Landsat Band 7 (2.08 to 2.35 μm , shortwave-infrared), respectively [26,40,41] (Table 1).

Differencing the NBR between pre- and post-fire scenes allows for isolating burned from unburned areas. The differenced NBR (dNBR) is defined as:

$$dNBR = NBR_{prefire} - NBR_{postfire} \quad (2)$$

A “relativized” version of the dNBR may be useful for removing bias effects of the pre-fire vegetative conditions. The relative differenced Normalized Burn Ratio (RdNBR) considers offset calculations for pre-fire landscape heterogeneity in vegetation condition [42]. The relative differenced Normalized Burn Ratio is defined as:

$$RdNBR = dNBR / \sqrt{ABS(NBR_{prefire}/1000)} \quad (3)$$

Satellite imagery access, pre-processing, and burn ratio calculations (dNBR and RdNBR) were conducted by the MTBS Project (www.MTBS.gov).

2.5. Data Analysis

We calculated summary statistics to describe burn severity using the CBI protocol. Correlation analysis was conducted to relate CBI to satellite burn classifications. We summarized the CBI data for all plots and by fire severity classes designated by the dNBR classification. CBI averages and ranges were described for each stratum. We calculated Pearson correlation values to test for relationships among strata scores, CBI, and satellite burn severity classifications (dNBR, RdNBR) for both IA and EA periods. Correlation and regression analysis were used to relate plot CBI values to overall vegetation changes for all plots and by burn severity class sub-groupings. Burn severity of grasslands is not well defined or understood. Based on the differences between grassland and woodland land-types and structure, fire behavior, fuel combustion and consumption, and directed heat effects (e.g., fires in grasslands affect greater proportion of ground and ground fuel strata compared to woodlands with varied

strata), it is possible that separate CBI reflectance models are needed for the different land-types. For these reasons, we developed separate predictive models of burn severity for grasslands and woodlands.

Regression models were compared among CBI and satellite burn severity classifications. We developed final regression models predicting dNBR and RdNBR using CBI. Model performance using linear and non-linear regression was compared based on model significance and r-square. Final regression model selections were based on model significance, r-square values, and normality of residuals. Final regression models were used to determine severity class threshold values for dNBR and RdNBR. Thresholds of severity classifications can be adapted to address many applications and, using the regression equations, CBI severity determinations can easily be converted to threshold values for dNBR and RdNBR [30]. We chose CBI threshold values that both signified observed changes in vegetation conditions and facilitated comparison of our results to those of other studies. These thresholds were: unburned (CBI = 0 to 0.1); low severity (0.1 to 1.24); moderate severity (1.25 to 2.24); and high severity (2.25 to 3.0). Reclassifications were done using the Classify command in ArcToolbox (ArcGIS 10.3).

Models of dNBR and RdNBR were compared based on model r-square values and confusion matrices that assessed classification accuracy. Confusion matrices showed the classification of field plots and remotely sensed pixels for each model. From confusion matrices we calculated the overall classification accuracy, user's accuracy, and producer's accuracy. Overall accuracy is the percentage of correct classifications across all burn severity classes, user's accuracy is the percentage of pixel values classified correctly in each burn severity class, and producer's accuracy represents the percentage of CBI plots classified correctly in each burn severity class. User's and producer's accuracies were developed for each burn severity class and compared. All statistical analyses and development of classifications were performed using SAS v 9.3 (Cary, NC, USA) statistical software package.

3. Results

3.1. Composite Burn Index (CBI)

CBI scores ranged from 0.05 to 2.94 with a mean value of 1.90. Grass was the only stratum scored on all plots while the tall tree stratum was scored on the fewest ($n = 14$). Among strata, all had CBI scores that spanned nearly the entire range of possible values (0 to 3.0). The shrub stratum showed the highest mean CBI score (2.27) while tall trees had the lowest (1.22). Scores of grass and shrub strata were consistently higher than their respective plot-level CBI scores. Although plots were stratified by severity classes prior to sampling (*i.e.*, 30 each of unburned, low, moderate, and high severity as classified in the dNBR EA (MTBS)), based on plot CBI scores of burned plots, we sampled 12 low severity plots (CBI ≤ 1.25), 52 moderate severity plots (CBI = 1.26 to 2.25), and 27 high severity plots (CBI > 2.26).

Rank patterns in stratum scores were similar for low and moderate severity conditions (Figure 3). Specifically, average stratum scores increased from the substrate layer to the shrub layer and then decreased to the tall tree layer. The tall tree layer had the lowest average strata score for low and moderate severities. For high severity plots, all strata had average CBI scores > 2.0 except for the tall tree stratum (mean score = 1.93) and, of these, the stratum scores of grass and shrub strata were the highest. Mean CBI values for low, moderate, and high classes increased with the severity classification. Similarly,

within the low, moderate, and high classes, each stratum’s mean CBI score also increased with severity (Figure 3).

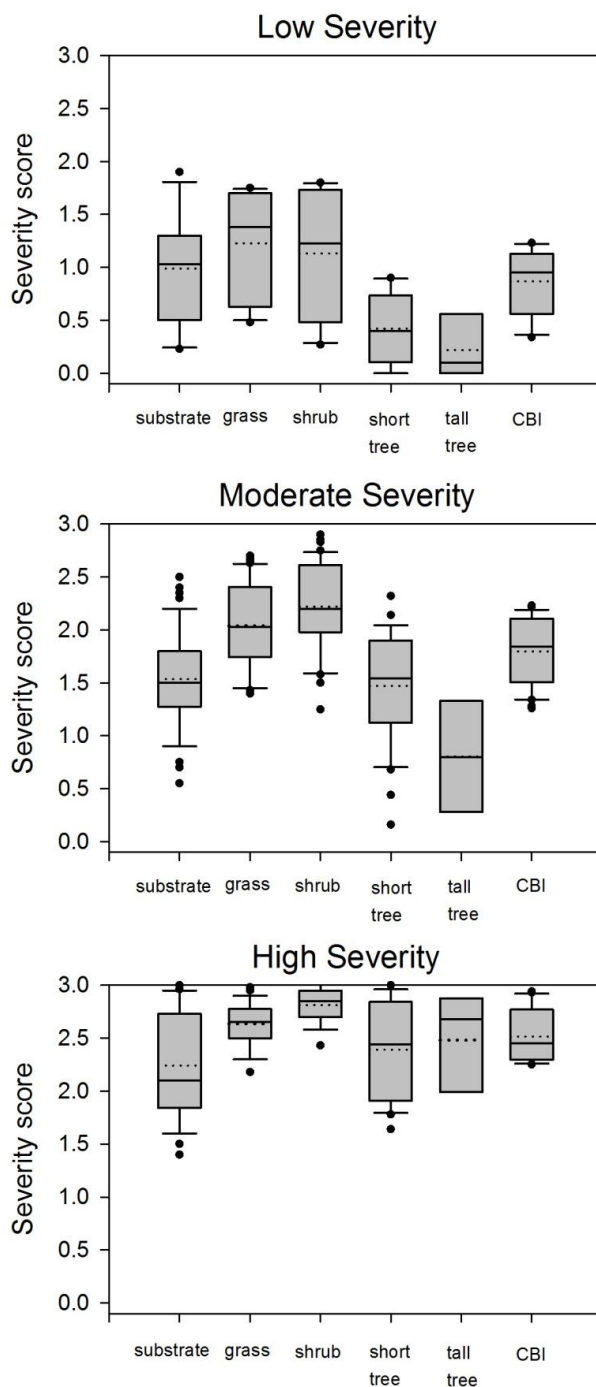


Figure 3. Box plots summarizing stratum scores and total plot CBI scores by severity class. Severity classes are determined by measured CBI scores of plots. The boundary of the box closest to zero indicates the 25th percentile, the line within the box marks the median, and the boundary of the box farthest from zero indicates the 75th percentile. Whiskers (error bars) above and below the box indicate the 90th and 10th percentiles. Means are represented by the dotted line.

Data distributions and means of CBI stratum scores followed similar patterns across land-types (Figure 4). Only data from woodlands spanned the full range of CBI scores in all strata (Figure 4). From

the substrate to the tall tree stratum, scores tended to increase to the shrub stratum and then decrease. Mean CBI scores for grasslands were always higher than the grassland substrate stratum scores and lower than shrub stratum scores. Mean and median scores for shrubs were generally greater than 2.0 while these scores for short trees were less than 2.0.

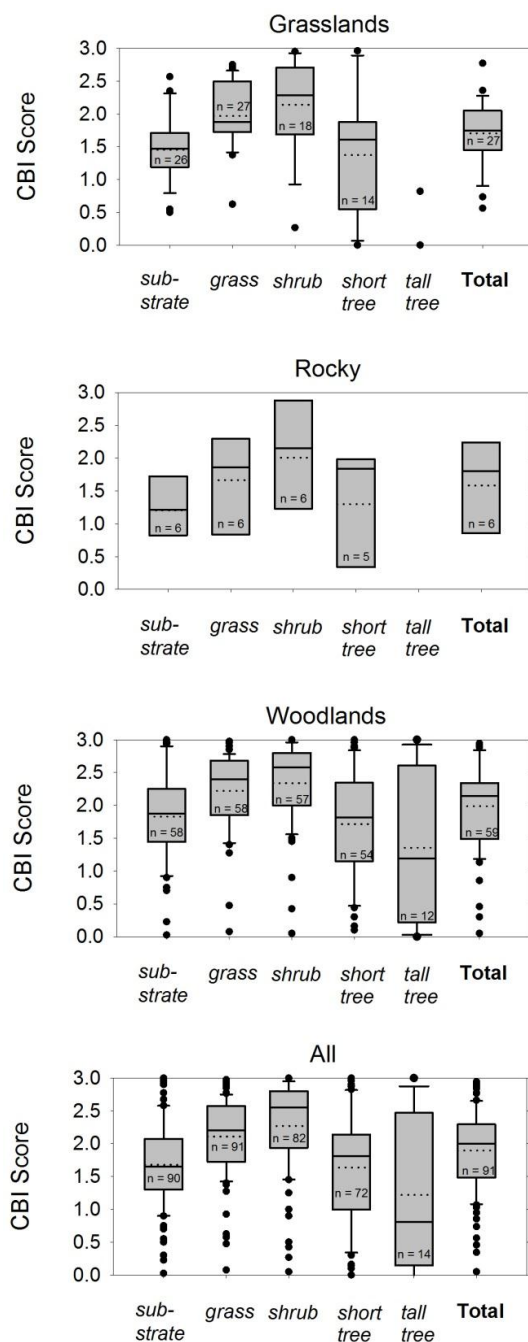


Figure 4. Box plots summarizing stratum scores and total plot CBI scores. Plots show differences in stratum scores by land-types and for all land-types combined. The boundary of the box closest to zero indicates the 25th percentile, the line within the box marks the median, and the boundary of the box farthest from zero indicates the 75th percentile. Whiskers (error bars) above and below the box indicate the 90th and 10th percentiles. Means are represented by the dotted line.

3.2. CBI and Satellite Classification

CBI was significantly correlated with all satellite-derived severity classifications regardless of assessment timing or interpolation use. CBI was most highly correlated with the IA dNBR severity classifications ($r = 0.78, p < 0.0001$; Table 2). The second-best relationship among CBI and satellite classifications existed with the IA RdNBR ($r = 0.76, p < 0.0001$). Across all strata, dNBR generally showed higher correlations with CBI than RdNBR (Table 2). The use of cell interpolation with satellite imagery classification of burn severity resulted in higher correlations among dNBR, RdNBR and CBI except for the case of dNBR in the EA.

Table 2. Pearson correlations (r), p -values (p), and sample sizes (n) among satellite-derived burn severity classifications and stratum scores and the composite burn index (CBI). Correlations do not include unburned plots.

			Substrate	Herb/Grass	Shrub	Short Tree	Tall Tree	CBI	
no cell interpolation	Initial	dNBR	r	0.48	0.43	0.42	0.46	0.63	0.74
			p	<0.0001	<0.0001	0.0001	<0.0001	0.0164	<0.0001
			n	90	91	81	73	14	120
		RdNBR	r	0.33	0.25	0.39	0.45	0.49	0.66
			p	0.0015	0.0151	0.0003	<0.0001	0.0783	<0.0001
			n	90	91	81	73	14	120
	Extended	dNBR	r	0.45	0.32	0.32	0.42	0.67	0.59
			p	<0.0001	0.0018	0.0033	0.0003	0.0081	<0.0001
			n	90	91	81	73	14	120
		RdNBR	r	0.41	0.30	0.32	0.40	0.72	0.18
			p	<0.0001	0.0037	0.0035	0.0004	0.004	0.0472
			n	90	91	81	72	14	91
interpolation	Initial	dNBR	r	0.51	0.43	0.43	0.48	0.59	0.78
			p	<0.0001	<0.0001	<0.0001	<0.0001	0.027	<0.0001
			n	90	91	81	73	14	120
		RdNBR	r	0.40	0.32	0.54	0.49	0.75	0.76
			p	<0.0001	0.0017	<0.0001	<0.0001	0.0021	<0.0001
			n	90	91	81	73	14	120
	Extended	dNBR	r	0.44	0.30	0.30	0.40	0.66	0.59
			p	<0.0001	0.0044	0.0064	0.0004	0.01	<0.0001
			n	90	91	81	73	14	120
		RdNBR	r	0.38	0.29	0.31	0.39	0.71	0.55
			p	0.0003	0.005	0.0053	0.0006	0.0045	<0.0001
			n	90	91	81	73	14	120

The use of cell interpolation did not necessarily improve correlations among satellite classifications and individual stratum scores. Strata were generally most highly correlated to satellite classifications (either dNBR or RdNBR) from the IA using interpolation. Among individual strata, the tall tree stratum was consistently the highest correlated with satellite classifications followed by substrate, and then the shrub stratum. (Table 2).

3.3. Predictive Models of Burn Severity and Thresholding

The ability of CBI to predict burn ratios was equal when comparing linear and non-linear models. Significant predictive models of both dNBR and RdNBR were made for the IA and EA periods (Table 3, Figure 5). Overall, best models occurred with the IA rather than the EA period. Examination and ground-truthing of IA models and maps, particularly of dNBR, suggested that satellite-derived burn severity in grassland land-types may be overestimated. Rocky plots were grouped with the woodlands since they typically supported trees. When separated by type, models utilizing data from woodlands performed better than those from grasslands. However, even models from grasslands were found to be significant (Table 3). Burn severity class threshold values were generally lower using dNBR versus RdNBR and higher for grasslands compared to woodlands (Table 4).

Table 3. Regression models of remotely sensed burn ratios and the composite burn index (CBI).

Variable	Parameter Estimate	SE	Probability > <i>t</i>	Model Probability > <i>F</i>	Adjusted <i>R</i> ²
All plots (n = 120)					
dNBR_IA				<0.001	0.61
Intercept	59.91863	16.93055	0.0006		
CBI	132.61502	9.76113	<0.0001		
RdNBR_IA				<0.001	0.57
Intercept	88.9992	49.41016	0.0742		
CBI	359.14602	28.48691	<0.0001		
dNBR_EA				<0.001	0.35
Intercept	-66.04456	28.40856	0.0056		
CBI	108.52425	13.49596	<0.0001		
RdNBR_EA				<0.001	0.30
Intercept	-79.28319	42.58894	0.0651		
CBI	173.74911	24.55421	<0.0001		
Woodlands (n = 86)					
dNBR_IA				<0.001	0.69
Intercept	50.92341	17.82425	0.0054		
CBI	137.77572	10.02647	<0.0001		
RdNBR_IA				<0.001	0.74
Intercept	40.5572	39.24262	0.3043		
CBI	341.74184	22.07469	<0.0001		
Grasslands (n = 34)					
dNBR_IA				<0.001	0.38
Intercept	89.38738	41.63793	0.0395		
CBI	114.00274	25.70259	0.0001		
RdNBR_IA				<0.001	0.47
Intercept	159.81218	134.76715	0.2444		
CBI	442.91999	83.19011	<0.0001		

Table 4. Burn severity classes and their corresponding CBI values, definitions, and threshold values. CBI values and definitions follow Miller and Thode [42] and were deemed appropriate for the study area. Threshold value determinations were based on regression models in Table 3.

Burn Severity Classes				
	Unchanged	Low	Moderate	High
CBI Values ^a	0 to 0.1	0.1 to 1.24	1.25 to 2.24	2.25 to 3.0
Definition	One year after the fire the area was indistinguishable from pre-fire conditions. This does not always indicate the area did not burn	Areas of surface fire occurred with little change in cover and little mortality of the structurally dominant vegetation	The area exhibits a mixture of effects ranging from unchanged to high severity within the scale of one pixel (30 m ²)	Vegetation has high to 100% mortality
All land-types				
Threshold values				
Initial Assessment				
dNBR *	73	225	358	
RdNBR	123	536	895	
Extended Assessment				
dNBR	-56	69	178	
RdNBR	-63	137	311	
Woodlands				
Initial Assessment				
dNBR †	64	222	360	
RdNBR	73	466	808	
Grasslands				
Initial Assessment				
dNBR	100	231	345	
RdNBR *	202	711	1154	

* = best prediction with CBI, † = best prediction with CBI for individual land-type models, ^a = CBI threshold values chosen so to be comparable to most studies

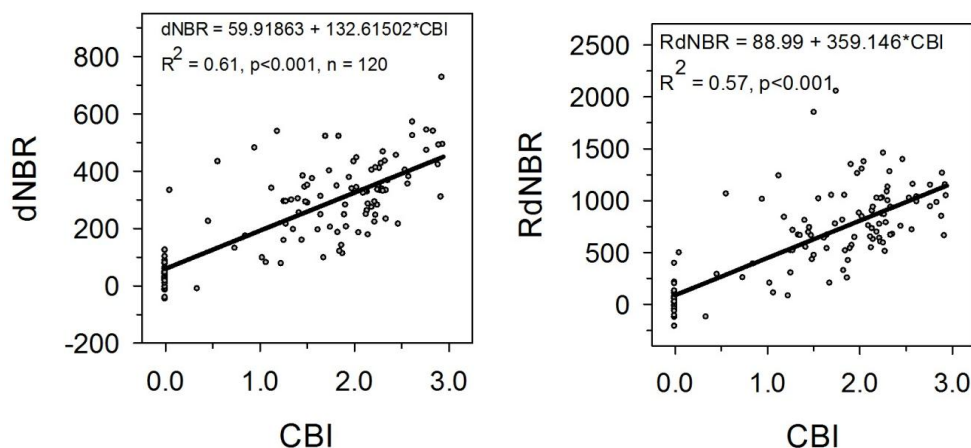


Figure 5. Scatterplots and regression models for initial assessment satellite imagery burn ratios predicting CBI from the full set of burned and unburned plots ($n = 120$). The use of non-linear models did not improve the predictive ability of regressions.

3.4. Accuracy Assessment

In general, the accuracy assessment of severity classifications did not reveal any model that excelled above all others. Accuracies generally seemed to be comparable to that of the MTBS classification; however these results may not be comparable due to different classification methods, particularly of the unburned areas. Overall model accuracies ranged from 37.5 to 44.2 percent using data from all land-types (Table 5). Overall accuracies of satellite classifications using IA dNBR, IA RdNBR, and EA dNBR were nearly equal (43% to 44%) while EA RdNBR was lower (37.5%). Compared to overall accuracies based on all land-types, accuracies were improved 4.4% to 11.6% by considering burn severity classification developed from woodlands only. Models considering just burn severity in grasslands had similar accuracies as those that consider all land-types. User's accuracies were highest for moderate and high severity classes and lowest for classifications of unburned conditions. For all land-types, user's accuracies of the high severity class were more accurately predicted by EA imagery, while moderate and low severity classes were more accurately predicted by IA imagery (Table 5). For woodlands, user's accuracy generally decreased from high to moderate to low severity classes. For grasslands, user's accuracies were greatest for moderate severity classes and lowest for high and low severity classes. Producer's accuracies (*i.e.*, the probability that a given fire severity class of a plot is classified as such) were lowest for unburned and high severity classes and greatest for low and moderate severity classes. Unburned class thresholds were typically only slightly outside of the dNBR and RdNBR ranges, but nonetheless were classified incorrectly. Producer's accuracies were mixed across burn severities for the different combinations of dNBR and RdNBR in initial and extended assessments. Compared to models based on all land-types, producer's accuracies were generally higher for models based only on woodlands and lower for models based on grasslands.

Table 5. Confusion matrices results showing the accuracies of the different methods/models produced. User's and producer's accuracies are divided into four burn severity classes; unb. (unburned), low, mod (moderate), and high. Overall accuracy of the MTBS classification method may be inflated since classification of some severity classes (e.g., unburned) did not follow the same methodology.

Method	Overall Accuracy	User's Accuracy				Producer's Accuracy			
		unb.	low	mod	high	unb.	low	mod	high
<i>All land-types</i>									
dNBR_IA	43.3	100.0	13.0	61.1	61.1	6.7	54.5	66.0	37.9
RdNBR_IA	44.2	-	16.7	60.3	53.3	0.0	63.6	76.0	27.6
dNBR_EA	43.3	100.0	10.9	57.4	90.9	6.7	45.5	70.0	34.5
RdNBR_EA	37.5	-	10.6	51.5	100.0	0.0	45.5	70.0	17.2
<i>Woodlands</i>									
dNBR_IA _{wood}	47.7	100.0	12.9	60.5	80.0	8.7	57.1	71.9	50.0
RdNBR_IA _{wood}	55.8	83.3	15.4	68.6	78.9	21.7	57.1	75.0	62.5
<i>Grasslands</i>									
dNBR_IA _{grass}	44.1	-	15.4	66.7	33.3	0.0	50.0	66.7	20.0
RdNBR_IA _{grass}	44.1	-	15.4	68.4	0.0	0.0	50.0	72.2	0.0
MTBS	-	-	19.4	65.6	57.1	-	54.5	42.0	55.2

4. Discussion

4.1. Application of CBI

This study quantified changes in oak woodland and grassland vegetation across a gradient of burn severities. The results of this study are new given that no known published information using the Landscape Assessment [26] is currently available from oak woodlands and only one other published study in the eastern U.S. exists from a site with a significant oak component [43]. FIREMON Landscape Assessment methods and applications are new for many managers and scientists in this region likely due to the lack of large-scale wildfires and federal lands compared to the western U.S. Methods and results presented here may help to refine and understand future burn severity and monitoring activities.

An impetus for this study was concern that burn severity classifications do not perform well in oak woodland and grassland vegetation. Burn severity classification in grasslands poses a concern because vegetation change detection has potential to underestimate burn severities despite observations that fire may alter the composition of grasslands (e.g., shift composition from native bunchgrass to forb and annual grass dominance) which may not be detected using satellite imagery. However, it is possible that the IA imagery could detect a level of ash or bare soil that would correlate with resulting, lagged effects in grassland or woodland composition. This could explain why CBI was generally more highly correlated with the IA than the EA. In a longleaf pine (*Pinus palustris*) ecosystem, Picotte and Robertson [31] note that some burn severity effects evident on the ground at the time of CBI sampling one year post fire were no longer detected by the EA imagery and as a result compared the IA and the EA with imagery taken at an intermediate time frame of three months.

A consequence of the lack of studies from the eastern U.S. that have utilized the Landscape Assessment methodology is that fire severity has been poorly defined with regard to changes in vegetation. By measuring the CBI at each plot we were able to identify strata changes associated with this burn severity classification scheme. Mean CBI scores were slightly higher for woodlands than grasslands. Though somewhat counterintuitive, mean CBI scores (Figure 4) in woodlands were higher than the means for both short and tall tree strata. For all land-types, mean scores of grass and shrub strata were consistently higher than the mean CBI while mean scores of substrate and short tree strata closely matched the mean CBI. Within grasslands, CBI scores were frequently higher than the substrate stratum score and lower than shrub stratum score. This suggests that the shrub stratum in the grasslands more readily achieved high severity effects and its scores generally elevated the CBI. In grasslands and open woodlands, there may be little opportunity to rate severity based on effects on woody cover change. However, where woody cover is present in grasslands, this may aid in better defining fire severity in grasslands, and may support the notion that ratings for grassland CBI scores are comparable to those of more forested areas and effects. Definitions and understanding of fire severity in grasslands are lacking, and therefore it is difficult to judge whether CBI methods are appropriate for grassland plots. A synthesis of fire severity and vegetation response is needed for grasslands similar to that presented by Keeley [13]. Based on our measurements, it appeared that most grassland plots had moderate burn severities and few fell within the ranges of low and high severity conditions.

We thought that to get a representative severity assessment using the CBI in short-statured oak woodlands (*i.e.*, Cross Timbers), we needed to modify the CBI strata. Stratum heights were developed

in western, coniferous forests [26] and we were concerned that the tree height break points did not fit the short tree stature and lack of canopy stratification that exists in woodlands and more open forest community structures. For example, little duff exists in the substrate strata of the WMWR, tall shrubs and short trees are largely composed of 1 to 3 m tall blackjack oak, and the overstory canopy is typically short (3 to 9 m) and rarely exceeds 9 m. For these reasons, we scaled the tree strata to what we perceived as an accurate representation of the pre-fire height stratification of these woodlands.

Miller and Thode [42] attempted a relativized change metric based on the heterogeneity of the unburned landscape leading to the development of the RdNBR and DeSantis and Chuvieco [44] tested modifications to the CBI for a similar reason; to weight severity scores by pre-fire cover. Both efforts attempted to scale or adapt broad change metrics to more localized conditions. We chose to modify the height categories for the tree strata, for the same purpose: to scale the burn index to local conditions. However, because we did not sample with a control to compare results of un-modified strata, we cannot say if scaling the stratum heights had any effect on the classification accuracy or predictive relationship among CBI and satellite classifications. Another discrepancy between the CBI protocol and its apparent fit to the xeric oak ecosystem of the south central U.S. occurred regarding char heights in that they were too high and not appropriately scaled to the short trees in the Cross Timbers (thus lowering the score for that stratum). For example, for intermediate and tall trees, low severity char height was 1.8 m, moderate severity was 2.8 m, and high severity was greater than 5 m. In many cases, to score the highest rating for the char height (*i.e.*, 3.0), char would have to be taller than the trees. This resulted in an incongruous score for char height relative to the other metrics in that stratum, and potentially had the effect of artificially lowering the severity score for that tree layer. To mitigate this problem in the future, if tree heights are modified, then char height modifications should perhaps also be considered.

4.2. Satellite Imagery Classification

Based on correlations among strata and satellite imagery classifications (Table 2), the tall tree stratum was most strongly related to satellite classifications, regardless of assessment timing, use of interpolation, or burn ratio (dNBR or RdNBR). The tall tree stratum was only measured on 14 of the 120 plots and this is likely to be a common rating frequency in short-statured forests and in open-structures in a mosaic of grasslands. The next best strata correlated with burn ratio were substrate and short tree. These strata were typically more highly correlated to burn ratios than the grass or shrub strata. All correlations among CBI and the substrate, grass, shrub, and short tree strata were greatest with the IA dNBR using interpolation; therefore we chose this burn ratio as the best-suited for predicting CBI.

CBI and burn ratio correlations were higher in woodlands than grasslands. Other studies have shown that performance and utility of remotely sensed burn severity may be limited in grassland-dominated regions [45]. The observation that dNBR was more highly correlated with CBI for all plots, but RdNBR was more highly correlated with woodlands and grasslands separately, suggests that the relationships among the two ratios and CBI differed by land-type. This was our premise for providing separate models and thresholds for woodlands and grasslands in Table 4. Regardless of which burn severity ratio is chosen, it should be expected that the majority of the variance in observed CBI can be explained.

Correlations among burn ratios and CBI were consistently higher for the IA compared to EA and this difference was consistent when separating correlations by strata (Table 2). Why would IA imagery better

predict burn severity when the timing of the measurement of burn severity matched the EA? Higher correlation between CBI and the IA imagery suggests that immediate post-fire changes detected by satellite remain identifiable by observers utilizing the CBI one year later, and/ or that “green-up” detected by EA imagery may mask post-fire effects detectable on the ground. The EA should provide additional data about delayed survival and mortality and, at this time, it is not clear why the EA is less useful for classifying severity. We hypothesize that it is related to the properties of grassland vegetation, their post-fire recovery, and reflectance.

IA models for dNBR and RdNBR explained 61 and 57 percent of the variance in CBI, respectively. Coefficients of determination (R^2) are comparable to or lower than the best model accuracies presented by Cansler and McKenzie [30] for the northern Cascades, Miller *et al.* [18] for sites in the Sierra Nevada and Klamath Mountains, Picotte and Robertson [31] for the southeastern U.S., and many other sites throughout the western U.S. (see Table 12 in Cansler and McKenzie [30] and Parks *et al.* [46]). Despite our models having similar explanatory power as many others, overall the classification accuracies were lower.

Accuracies of burn classifications were much lower in unburned (user’s accuracy) and low severity classes (producer’s accuracy) compared to moderate and high severity classes. Accuracies of moderate and high severity classifications were comparable to those reported in other studies. It appears that the cause for the inaccuracy of unburned/low severity areas was that many of the unburned plots had image classified burn ratios in the range of low severity values. This situation is a case where a regression only approach to deriving class thresholds could be supplemented and improved with slight adjustments. In this case, classifications between unburned and low severity classes could be improved by increasing IA threshold values to around 140 for dNBR and 320 for RdNBR. These values would be on the high range for unburned/low severity threshold values compared to other sites throughout the western U.S. (see Table 13 in Cansler and McKenzie [30] and Parks *et al.* [46]). Based on the data, it is not clear why increasing these threshold values for dNBR and RdNBR is needed and whether similar results would be found in comparable conditions or vegetation. Differences in conditions (e.g., spatial, temporal, radiometric, and geographic) of two image scenes can affect fire severity quantification [29]. Further, it is possible that the need to increase threshold values is because changes on unburned plots are higher than typically observed due to the added effects of exceptional drought on vegetation conditions. Combined drought and fire effects influencing CBI is an example for why thresholds can vary between burns and thresholding may be needed for each fire. Further work could be done to refine threshold points and increase accuracies by including ground-truthing sites near mapped break points.

Classification of high burn severity had the highest user’s accuracy while classification of moderate burn severity had the highest producer’s accuracy. Other studies have shown higher classification accuracies with increased severity. Depending on application, it may be that the accuracy of the burn severity classification is adequate for specific situations such as distinguishing moderate to high severity classes. Considering the accuracy of the woodland only model, it seems that woodland burn severity classification should be reliable, particularly for classifying moderate to high severity conditions. Based on the accuracy differences between woodlands and grasslands (Table 5), it would seem that much of the inaccuracy of classifying “All land-types” is likely to be due to classifying grasslands. Efforts to improve models and classification of grassland burn severity may consider modifications to the burn rating system (e.g., CBI), imagery processing approaches (*i.e.*, scene timing), and classification methodology.

4.3. Recommended Methods for Validating Future Fire Severity Maps in Oak Woodlands

Recommendations for future work are based solely on our findings from this single fire. Ideally, more studies would be available to compare the results over replications. Considering this, we would recommend using an unaltered CBI protocol paired with the IA period burn severity imagery (dNBR or RdNBR). In the Cross Timbers region it is highly likely that the tall tree class will not be rated using the standard CBI form. CBI—Satellite relationships will likely be best for strata that capture the dominant overstory layer, particularly for woodlands. Areas with higher percentages of woody cover are likely to be more accurately classified than those dominated by grasslands. In many parts of the eastern U.S. high severity burns are uncommon and occur during drought conditions. Burn severity monitoring should consider the non-fire related effects, such as drought, and how much they may contribute to the overall variability in vegetation observed.

5. Conclusions

Our findings suggest that dNBR and RdNBR reflectance data, thresholded using total CBI, particularly from the IA period, produces the most accurate burn severity map in oak woodlands. To our knowledge, this paper presents one of the most rigorous analyses of burn severity in eastern U.S. deciduous forests and is the first time that remotely sensed information has been used to develop burn severity thresholds and maps in oak-dominated woodlands including a gradient to grassland vegetation. The accuracy of burn severity models (Table 5) suggests that burn severity metrics have greatest utility for monitoring fire effects to woodlands and, less so, in grasslands. The lowered accuracies of classifications of grasslands (*i.e.*, non-woody areas) beg the question: What are definitions of burn severity for grass/ herbaceous dominated areas, particularly in situations where they occur within a matrix of woodlands? Further advancements in burn severity monitoring in eastern U.S. vegetation types, including improved detection of substrate and grass strata change, would both improve our understanding of their fire ecology and significantly enhance documentation and monitoring through remote sensing.

Acknowledgments

This research was funded by the U.S. Fish & Wildlife Service. We thank Paige Schmidt, Walter Munsterman, Dan McDonald, and Jeremy Dixon of the (U.S. Fish and Wildlife Service) for their assistance in study design, training, and fieldwork. Nate Benson (National Park Service) provided critical guidance regarding CBI data collection and analysis and helpful review comments on previous versions of this manuscript. Stephen Howard (USGS Center for Earth Resources Observation and Science (EROS)) graciously provided the extended assessment satellite classification data. Fieldwork assistance was provided by Carter Kinkead, Matt Bourscheidt, Ryan Simms, Jonathan Hogg, Michael Womack, Ian Dudley, Michael Johnson, Chris Burgess, and Lydia Tomlinson. The findings and conclusions in this article are those of the authors and do not necessarily represent the views of the US Fish and Wildlife Service.

Author Contributions

Michael Stambaugh conceived study, designed sampling, conducted the analysis, wrote the paper; Lyndia Hammer conceived study, designed sampling, collected data, and contributed to writing the paper; Ralph Godfrey conceived study, designed sampling, collected data, and contributed to writing the paper.

Conflicts of Interest

The authors declare no conflict of interest.

References

1. De Santis, A.; Chuvieco, E. Burn severity estimation from remotely sensed data: Performance of simulation *versus* empirical models. *Remote Sens. Environ.* **2007**, *108*, 422–425.
2. Boer, M.M.; Macfarlane, C.; Norris, J.; Sadler, R.J.; Wallace, J.; Grierson, P.F. Mapping burned areas and burn severity patterns in SW Australian eucalypt forest using remotely-sensed changes in leaf area index. *Remote Sens. Environ.* **2008**, *112*, 4358–4369.
3. Wang, Z.; Jiang, L.; Kong, B.; Chen, H.; Zhang, T. Remote sensing measure of severity on the Zhalong wetlands and consequent ecological effects. In Proceedings of the Third International Workshop on Earth Observation and Remote Sensing Applications, Changsha, China, 11–14 June 2014.
4. Salvia, M.; Ceballos, D.; Grings, F.; Karszenbaum, H.; Kandus, P. Post-fire effects in wetland environments: Landscape assessment of plant coverage and soil recovery in the Paran áRiver delta marshes, Argentina. *Fire Ecol.* **2012**, *8*, 17–37.
5. Wiens, J.; Sutter, R.; Anderson, M.; Blanchard, J.; Barnett, A.; Aguilar-Amuchastegui, N.; Avery, C.; Laine, S. Selecting and conserving lands for biodiversity: The role of remote sensing. *Remote Sens. Environ.* **2009**, *113*, 1370–1381.
6. Kulakowski, D; Veblen, T.T. Effect of prior disturbances on the extent and severity of wildfire in Colorado subalpine forests. *Ecology* **2007**, *88*, 759–769.
7. Perry, D.A.; Hessburg, P.F.; Skinner, C.N.; Spies, T.A.; Stephens, S.L.; Taylor, A.H.; Franklin, J.F.; McComb, B.; Riegel, G. The ecology of mixed severity fire regimes in Washington, Oregon, and Northern California. *Forest Ecol. Manag.* **2011**, *262*, 703–717.
8. Koldan, C.A; Rogan, J. Mapping wildfire burn severity in the Arctic Tundra from downsampled MODIS data. *Arct. Antarct. Alp. Res.* **2013**, *45*, 64–76.
9. Twidwell, D.T.; Rogers, W.E.; McMahan, E.A.; Thomas, B.R.; Kreuter, U.P.; Blankenship, T.L. Prescribed extreme fire effects on richness and invasion in coastal prairie. *Invasive Plant Sci. Manag.* **2012**, *5*, 330–340.
10. Williams, M.A.; Baker, W.L. Spatially extensive reconstructions show variable-severity fire and heterogeneous structure in historical western United States dry forests. *Glob. Ecol. Biogeogr.* **2012**, *21*, 1042–1052.
11. Ful é, P.Z.; Swetnam, T.W.; Brown, P.M.; Falk, D.A.; Peterson, D.L.; Allen, C.D. Unsupported inferences of high severity fire in historical western United States dry forests: Response to Williams and Baker. *Glob. Ecol. Biogeogr.* **2013**, *23*, 825–830.

12. Ryan, K.C.; Noste, N.V. Evaluating prescribed fires. In Proceedings of the Symposium and Workshop on Wilderness Fire, Missoula, MT, USA, 15–18 November 1983.
13. Keeley, J.E. Fire intensity, fire severity and burn severity: A brief review and suggested usage. *Int. J. Wildland Fire* **2009**, *18*, 116–126.
14. Morgan, P.; Keane, R.E.; Dillon, G.K.; Jain, T.B.; Hudak, A.T.; Karau, E.C.; Sikkink, P.G.; Holden, Z.A.; Strand, E.K. Challenges of assessing fire and burn severity using field measures, remote sensing and modelling. *Int. J. Wildland Fire* **2014**, *23*, 1045–1060.
15. Stroppiana, D.; Azar, R.; Calò, F.; Pepe, A.; Imperatore, P.; Boschetti, M.; Silva, J.M.N.; Brivio, P.; Lanari, R. Integration of optical and SAR data for burned area mapping in Mediterranean regions. *Remote Sens.* **2014**, *7*, 1320–1345.
16. Pierce, A.D.; Farris, C.A.; Taylor, A.H. Use of random forests for modeling and mapping forest canopy fuels for fire behavior analysis in Lassen Volcanic National Park, California, USA. *Forest Ecol. Manag.* **2012**, *279*, 77–89.
17. Bolton, D.K.; Coops, N.C.; Wulder, M.A. Characterizing residual structure and forest recovery following high-severity fire in the western boreal of Canada using Landsat time-series and airborne LiDAR data. *Remote Sens. Environ.* **2015**, *163*, 48–60.
18. Miller, J.D.; Knapp, E.E.; Key, C.H.; Skinner, C.N.; Isbell, C.J.; Creasy, R.M.; Sherlock, J.W. Calibration and validation of the relative differenced Normalized Burn Ratio (RdNBR) to three measures of fire severity in the Sierra Nevada and Klamath Mountains, California, USA. *Remote Sens. Environ.* **2009**, *113*, 645–656.
19. Hessburg, P.F.; Agee, J.K.; Franklin, J.F. Dry forests and wildland fires of the inland Northwest USA: Contrasting the landscape ecology of the pre-settlement and modern eras. *Forest Ecol. Manag.* **2005**, *211*, 117–139.
20. Prichard, S.J.; Kennedy, M.C. Fuel treatments and landform modify landscape patterns of burn severity in an extreme fire event. *Ecol. Appl.* **2014**, *24*, 571–590.
21. Wimberly, M.C.; Cochrane, M.A.; Baer, A.D.; Pabst, K. Assessing fuel treatment effectiveness using satellite imagery and spatial statistics. *Ecol. Appl.* **2009**, *19*, 1377–1384.
22. Miller, J.D.; Safford, H.D. Trends in wildfire severity 1984–2010 in the Sierra Nevada, Modoc Plateau and southern Cascades, California, USA. *Fire Ecol.* **2012**, *8*, 41–57.
23. Parks, S.A.; Miller, C.; Nelson, C.R.; Holden, Z.A. Previous fires moderate burn severity of subsequent wildland fires in two large western US wilderness areas. *Ecosystems* **2014**, *17*, 29–42.
24. Johnstone, J.F.; Rupp, T.S.; Olson, M.; Verbyla, D. Modeling impacts of fire severity on successional trajectories and future fire behavior in Alaskan boreal forests. *Landsc. Ecol.* **2011**, *26*, 487–500.
25. Russell, R.E.; Saab, V.A.; Dudley, J.G. Habitat-suitability models for cavity-nesting birds in a postfire landscape. *J. Wildl. Manag.* **2007**, *71*, 2600–2611.
26. Key, C.H.; Benson, N.C. Landscape Assessment (LA): Sampling and analysis methods. In *FIREMON: Fire Effects Monitoring and Inventory System*; Lutes, D.C., Keane, R.E., Caratti, C.H., Key, N.C., Sutherland, S., Eds.; Rocky Mountain Research Station, USDA Forest Service: Fort Collins, CO, USA, 2006; p. 51.
27. Montealegre, A.L.; Lamelas, M.T.; Tanase, M.A.; de la Riva, J. Forest fire severity assessment using ALS data in a mediterranean environment. *Remote Sens.* **2014**, *6*, 4240–4265.

28. Tanase, M.A.; Santoro, M.; Wegmüller, U.; de la Riva, J.; Pérez-Cabello, F. Properties of X-, C- and L-band repeat-pass interferometric SAR coherence in Mediterranean pine forests affected by fires. *Remote Sens. Environ.* **2010**, *114*, 2182–2194.
29. Key, C.H. Ecological and sampling constraints on defining landscape fire severity. *Fire Ecol.* **2006**, *2*, 34–59.
30. Cansler, C.A.; McKenzie, D. How robust are burn severity indices when applied in a new region? Evaluation of alternate field-based and remote-sensing methods. *Remote Sens.* **2012**, *4*, 456–483.
31. Picotte, J.J.; Robertson, K.M. Validation of remote sensing of burn severity in south-eastern US ecosystems. *Int. J. Wildl. Fire* **2011**, *20*, 453–464.
32. Buck, P. Relationships of the woody vegetation of the Wichita Mountains Wildlife Refuge to geological formations and soil types. *Ecology* **1964**, *45*, 336–344.
33. National Climate Data Center (NCDC). Monthly Surface Data. National Climate Data Center, Asheville, North Carolina, USA. 1999. Available online: <http://www.ncdc/noaa.gov/> (accessed on 28 May 2009).
34. Stambaugh, M.C.; Marschall, J.M.; Guyette, R.P. Linking fire history to successional changes of xeric oak woodlands. *Forest Ecol. Manag.* **2014**, *320*, 83–95.
35. Hammer, L.D.; Stambaugh, M.C. Environmental gradients and controls of eastern redcedar (*Juniperus virginiana* L.) expansion from ancient refugia. *Biol. Invasions* **2015**, in press.
36. U.S. Drought Monitor. 2013. Available online: <http://droughtmonitor.unl.edu/monitor.html> (accessed on 9 July 2013).
37. Gesch, D.; Evans, G.; Mauck, J.; Hutchinson, J.; Carswell, W.J., Jr. The National Map—Elevation: U.S. Geological Survey Fact Sheet 2009-3053. Available online: <http://ned.usgs.gov> (accessed on 1 April 2015).
38. Hoagland, B. The vegetation of Oklahoma: A classification for landscape mapping and conservation planning. *Southwest. Nat.* **2000**, *45*, 385–420.
39. Eidenshink, J.; Schwind, B.; Brewer, K.; Zhu Z.L.; Quayle, B.; Howard, S. A project for monitoring trends in burn severity. *Fire Ecol.* **2007**, *3*, 3–21.
40. Key, C.H.; Benson, N.C. Measuring and remote sensing of burn severity: The CBI and NBR. In Proceedings of the Joint Fire Science Conference and Workshop, Boise, ID, USA, 15–17 June 1999.
41. Brewer, C.K.; Winne, J.C.; Redmond, R.L.; Opitz, D.W.; Mangrich, M.V. Classifying and mapping wildfire severity: A comparison of methods. *Photogramm. Eng. Remote Sens.* **2005**, *71*, 1311–1320.
42. Miller, J.D.; Thode, A.E. Quantifying burn severity in a heterogeneous landscape with a relative version of the delta Normalized Burn Ratio (dNBR). *Remote Sens. Environ.* **2007**, *109*, 66–80.
43. Wimberly, M.C.; Reilly, M.J. Assessment of fire severity and species diversity in the southern Appalachians using Landsat TM and ETM+ imagery. *Remote Sens. Environ.* **2007**, *108*, 189–197.
44. De Santis, A.; Chuvieco, E. GeoCBI: A modified version of the Composite Burn Index for the initial assessment of the short-term burn severity from remotely sensed data. *Remote Sens. Environ.* **2009**, *113*, 554–562.

45. Roy, D.P.; Boschetti, L.; Trigg, S.N. Remote sensing of fire severity: assessing the performance of the normalized burn ratio. *IEEE Geosci. Remote Sens. Lett.* **2006**, *3*, 112–116.
46. Parks, S.A.; Dillon, G.K.; Miller, C. A new metric for quantifying burn severity: The relativized burn ratio. *Remote Sens.* **2014**, *6*, 1827–1844.

© 2015 by the authors; licensee MDPI, Basel, Switzerland. This article is an open access article distributed under the terms and conditions of the Creative Commons Attribution license (<http://creativecommons.org/licenses/by/4.0/>).